2008 American Control Conference
Westin Seattle Hotel, Seattle, Washington, USA
June 11-13, 2008

Adaptive Camera Calibration With Measurable Position of Fixed Features

Apoorva Kapadia, David Braganza, Darren M. Dawson, and Michael L. McIntyre

Abstract: In this paper, a novel self-calibration method is developed for a camera attached to a mechanical system with known kinematics. An innovative least squares estimator is developed to compute the unknown intrinsic and extrinsic camera calibration parameters while an adaptive parameterized error prediction formulation is presented to compensate for the unknown pixel coordinates of the static objects projection. The estimator is based on a Lyapunov stability analysis which verifies convergence of the signals provided a persistent excitation condition is satisfied. Simulation results with and without additive pixel noise are also provided to illustrate the performance and robustness of the algorithm.

I. INTRODUCTION

With the advent of computer vision, camera calibration has become a fundamental research problem. From the broad perspective of computer vision, there are two aspects of camera calibration that have to be addressed, that of the cameras intrinsic parameters, specifically its geometric and optical characteristics, and its extrinsic attributes, given by its position and orientation in space. The intrinsic specifications are scale factors for each axis, coordinates of the image planes origin and the intersection of the optical axis with the image plane. The Euclidean transformation that yields the camera image frames 3-dimensional position and orientation in space with respect to the fixed world frame represents the extrinsic characteristics of the camera system and is independent of the cameras intrinsic parameters as described by [1].

Most of the previously published calibration methods predominantly looked at solving the hand-eye extrinsic calibration problem or the intrinsic calibration problem separately. algorithms that look at determining the position and orientation of a mounted camera with respect to the robot end-effector, observe the motion of the camera while the robot moves. The relationship between the end-effector and the camera is then described by a homogenous transform $AX = XB$, where A and B are matrices representing the change in end-effector and camera position respectively, while X is the unknown transform representing the extrinsic parameters, a problem first conveyed by Shiu & Ahmad [2]. Young $et\ al.$ [3] used a Denavit-Hartenberg model of the manipulator to simplify the problem, while Park & Martin [4] found a solution using Lie theory and least squares. Remy $et\ al.$ [5] solved for the extrinsic parameters as well as simultaneously determining the structure of the calibration object, while Li [6] decomposed the transformation matrix into its rotational and translational components resulting in two independent equations which could be solved separately.

Quaternions were used by Dornaika & Horaud [7] to derive a linear solution for the $AX = ZB$ problem, a modification of the previously described homogenous transform. In this case, a gripper was used as an end-effector along with the camera, where X represented the transform from the gripper to the camera while Z denoted the robot-world frame transformation. Strobl & Hirzinger [8] used a stochastic model to estimate the transformation for both versions of the homogenous equation and Zhao & Liu [9] described a screw theory solution. It is seen that most extrinsic calibration methods attempt to linearize the system models allowing for the use of various optimization and estimation techniques to reach a closed-form solution.

Brown [10] and Faig [11] were among the first to discuss the computation of intrinsic parameters. Sinc then, most methods involve the observation of a simple planar pattern described by Zhang [12], whose algorithm requires no constraint on the motion of the camera. Stein [13] employed a nonlinear search to predict the motion of feature points in a set of images from a camera that had undergone a known rotation. Nakazawa $et\ al.$ [14] described a cue-based method that calibrated the internal parameters of the camera while also estimating the structure of the 3-D object being projected, and Frahm $et\ al.$ [15] demonstrated a linearized form of the intrinsic parameter problem for a rotating camera.

Over time, the idea of self-calibration initially proposed by Faugeras & Maybank [16] has taken prominence due to the ease of application, reduced complexity and lower computational and equipment costs as the method requires little or no knowledge of the enviroments structure in the cameras field-of-view. The authors explained the use of epipolar transformations that could be recovered when the camera underwent a displacement. This work, along with Tsai [17] is possibly the first instance where the intrinsic and extrinsic parameters for a camera system were computed simultaneously. Additionally, exhaustive literature can be found including, but not restricted to [14], [18], [19] and [15].

This work is supported in part by a DOE Contract and a Honda Corporation Grant.

Contact Author: A. Kapadia is with the Department of Electrical & Computer Engineering, Clemson University, Clemson, SC 29634-0915 (akapadi@clemson.edu).
D. M. Dawson is with the Department of Electrical & Computer Engineering, Clemson University, Clemson, SC 29634-0915 (darren.dawson@ces.clemson.edu).
D. Braganza is with OFS, 50 Hall Road, Sturbridge, MA 01566 (dbragan@ofsoptics.com).
M. McIntyre is with the Department of Electrical Engineering, Western Kentucky University, Bowling Green, KY 42101-1082 (michael.mcintyre1@wku.edu).

978-1-4244-2079-7/08/$25.00 ©2008 AACC.

Unlike the works described before, the self-calibration algorithm described in this paper employs the nonlinear system equation along with the measured mechanical system[1] position and the known position of fixed object features to provide a least squares solution for the extrinsic and intrinsic parameters of the camera system. Because of the structure of the parameterizd pixel coordinate equation, an atypical nonlinear adaptive predictive error formula is proposed based on the methodology shown in [20]. Upon satisfaction of the persistent excitation condition, a Lyapunov-based stability technique verifed convergence of the estimation.

In this paper, Section 2 briefly explains the pinhole camera model and outlines the development of the geometric model relating the images pixel coordinates to the Euclidean coordinates of the feature points along with the transformation from the robot world frame to the camera frame. Section 3 details the prediction error formulation for every features pixel coordinates along with a least squares estimation law. Simulation results are shown in Section 4 for the cases with and without additive pixel noise to highlight the robustness of our estimation algorithm and Section 5 concludes the paper.

II. Model Development

A. An Overview of the Pinhole Camera Model

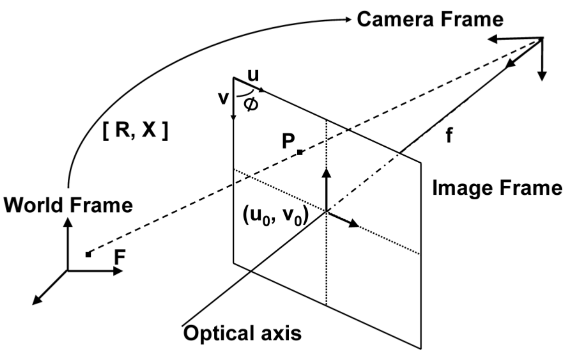

Fig. 1. The pinhole camera model

Figure 1 shows a simple pinhole camera model with a feature point whose Euclidean coordinates in the world frame are given by $F \in \mathbb{R}^3$, resulting in projected pixel coordinates $P \in \mathbb{R}^3$ on the image plane. The world frame is related to the camera frame by a rotation and translation, thus the relationship between the feature point, F and the pixel coordinates, P can be given by

$$P = A \left[\begin{array}{c} R, X \end{array} \right] F, \tag{1}$$

where $R \in SO(3)$ and $X \in \mathbb{R}^3$ are the extrinsic camera calibration parameters, representing the rotation and translation of the camera frame combined together to form $[R, X] \in \mathbb{R}^{4\times 3}$. In (1), $A \in \mathbb{R}^{3\times 3}$ is the intrinsic camera calibration matrix such that

$$A = \begin{bmatrix} fk_u & fk_u \cot\phi & u_0 \\ 0 & \frac{fk_v}{\sin\phi} & v_0 \\ 0 & 0 & 1 \end{bmatrix} \tag{2}$$

where $u_0 \in \mathbb{R}$ and $v_0 \in \mathbb{R}$ represent the pixel coordinates of the principal point, $k_u \in \mathbb{R}$ and $k_v \in \mathbb{R}$ represent the number of pixels per unit distance along the image axes u and v respectively. The focal length is denoted by $f \in \mathbb{R}$ and $\phi \in \mathbb{R}$ represents the angle between the image axes u and v.

B. Geometric Model

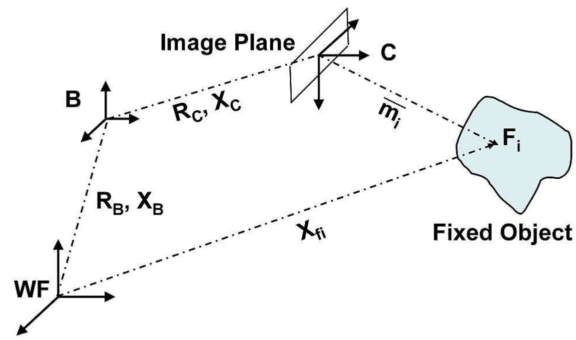

Fig. 2. Geometric relationships between the mechanical system, camera and fixed object.

In order to obtain accurate position information of the moving camera, it is mounted on a mechanical system, represented by B, whose fixed base frame is denoted by WF. Let $R_B(t) \in SO(3)$ and $X_B(t) \in \mathbb{R}^3$ denote the known rotation matrix and translation vector, respectively from B to WF, expressed in WF which can be computed from the system kinematics. Let the frame C represent the camera mounted onto the mechanical system, while $R_C \in SO(3)$ and $X_C \in \mathbb{R}^3$ represent the constant unknown rotation matrix and translation vector respectively, from C to B and are expressed in B.

The feature points of the fixed object are denoted by $F_i\ \forall i = 1, \ldots, n$ and the coordinates of the i^{th} feature point are denoted by the constant $X_{fi} \in \mathbb{R}^3$ relative to the base frame WF, and by the variable $\overline{m}_i(t) \in \mathbb{R}^3$ relative to the moving camera frame C, which is defined as follows

$$\overline{m}_i = \left[\begin{array}{ccc} x_i & y_i & z_i \end{array} \right]^T \tag{3}$$

where $x_i(t)$, $y_i(t)$ and $z_i(t) \in \mathbb{R}$ represent the coordinates of the i^{th} feature point relative to C. For the model development, it is assumed that the object is always in the cameras field-of-view, hence the distances of the feature points from the origin of C are always positive. Let $P_i(t) \in \mathbb{R}^3$ represent the pixel coordinates of the i^{th} feature point projected on the two-dimensional image in the C frame such that

$$P_i = \left[\begin{array}{ccc} u_i & v_i & 1 \end{array} \right]^T \tag{4}$$

with u_i and $v_i \in \mathbb{R}$ being the projected pixel coordinates for the i^{th} feature point. These coordinates are related to

[1]The term "mechanical system" represents robot manipulators, unmanned airborne or underwater vehicles, mobile robots or any similar systems

the normalized Euclidean coordinates by the pinhole camera model such that

$$P_i = \frac{1}{z_i} A\, \overline{m}_i \tag{5}$$

where, from (1), $A \in \mathbb{R}^{3\times3}$ is the unknown intrinsic camera calibration matrix which we assume has the form

$$A = \begin{bmatrix} a_{11} & a_{12} & a_{13} \\ 0 & a_{22} & a_{23} \\ 0 & 0 & 1 \end{bmatrix}. \tag{6}$$

III. Estimator Development

A. Prediction Error Formulation

From Figure 2, the relationship between the various coordinate frames can be represented as

$$R_B^T (X_{fi} - X_B) = R_C \overline{m}_i + X_C. \tag{7}$$

Using the unitary property of rotation matrices as seen in [21], where $R^T = R^{-1}$, (7) can be reorganized into

$$\overline{m}_i = R_C^T\, R_B^T (X_{fi} - X_B) - R_C^T X_C. \tag{8}$$

Thus, by substituting (8) in (5), the pixel coordinates, $P_i(t)$ can be expressed in terms of the robot kinematics, $R_B(t)$ and $X_B(t)$, the unknown extrinsic calibration parameters, R_C and X_C, and the coordinates of the object in the world frame, X_{fi}, as

$$P_i = \frac{1}{z_i} A \left(R_C^T R_B^T (X_{fi} - X_B) - R_C^T X_C \right). \tag{9}$$

Equation (9) can be further simplified to take the general form including a combined matrix similar (1), such that

$$P_i = \frac{1}{z_i} A \begin{bmatrix} R, T \end{bmatrix} \overline{X}_i \tag{10}$$

where,

$$T \triangleq -R_C^T X_C \in \mathbb{R}^3 \tag{11}$$

$$\overline{X_i} \triangleq \begin{bmatrix} \left(R_B^T (X_{fi} - X_B)\right)^T & 1 \end{bmatrix}^T \in \mathbb{R}^4 \tag{12}$$

$$R \triangleq R_C^T \in S0(3). \tag{13}$$

Equations (6), (11), and (13) represent the unknown camera calibration parameters that have to be determined. It can be seen that (9) contains the known variables $R_B(t)$, $X_B(t)$ and the Euclidean coordinates X_{fi} along with the unknown calibration parameters A, R_C and X_C. Thus $P_i(t)$ can be rewritten in its parameterized form as

$$P_i = \frac{1}{W_{zi}\theta_z} W_{xi}\theta_x \tag{14}$$

where $W_{xi}(t) \in \mathbb{R}^{3\times12}$ and $W_{zi}(t) \in \mathbb{R}^{1\times4}$ are the known regression matrices for the i^{th} feature point containing various combinations of elements of the known variables $R_B(t)$ and $X_B(t)$, with X_{fi} known *a priori*. The parameters $\theta_x \in \mathbb{R}^{12}$ and $\theta_z \in \mathbb{R}^4$ are the unknown constant vectors containing combinations of elements from A, R_C and X_C, which have to be estimated, such that

$$W_{xi}\theta_x = A \begin{bmatrix} R, T \end{bmatrix} \overline{X}_i, \tag{15}$$

$$W_{zi}\theta_z = \left\{ \begin{bmatrix} R, T \end{bmatrix} \overline{X}_i \right\}_3. \tag{16}$$

Let $\hat{P}_i(t) \in \mathbb{R}^3$ be the estimate of $P_i(t)$, with $\hat{\theta}_x(t)$ and $\hat{\theta}_z(t)$ representing unknown estimates of the constant parameter vectors θ_x and θ_x such that

$$\hat{P}_i = \frac{1}{W_{zi}\hat{\theta}_z} W_{xi}\hat{\theta}_x. \tag{17}$$

By reordering (14) and (17), it can be seen that

$$P_i W_{zi}\theta_z = W_{xi}\theta_x \tag{18}$$

$$\hat{P}_i W_{zi}\hat{\theta}_z = W_{xi}\hat{\theta}_z. \tag{19}$$

While subtracting (19) from (18) yields

$$P_i W_{zi}\theta_z - \hat{P}_i W_{zi}\hat{\theta}_z = W_{xi}\theta_x - W_{xi}\hat{\theta}_x \tag{20}$$

which can be rewritten as [22]

$$\tilde{P}_i = \frac{1}{W_{zi}\theta_z} \left(W_{xi}\tilde{\theta}_x - \hat{P}_i W_{zi}\tilde{\theta}_z \right) \tag{21}$$

where $\tilde{P}_i(t) \in \mathbb{R}^3$, $\tilde{\theta}_x(t) \in \mathbb{R}^{12}$ and $\tilde{\theta}_z(t) \in \mathbb{R}^4$ can be defined as the estimation errors as follows

$$\tilde{P}_i \triangleq P_i - \hat{P}_i; \quad \tilde{\theta}_x \triangleq \theta_x - \hat{\theta}_x; \quad \tilde{\theta}_z \triangleq \theta_z - \hat{\theta}_z.$$

After separating the known and unknown parameters, the expression in (21) can be rewritten as follows

$$\tilde{P}_i = \frac{1}{W_{zi}\theta_z} \begin{bmatrix} W_{xi} & -\hat{P}_i W_{zi} \end{bmatrix} \begin{bmatrix} \tilde{\theta}_x \\ \tilde{\theta}_z \end{bmatrix} \tag{22}$$

and can be further simplified as

$$\tilde{P}_i = \frac{1}{W_{zi}\theta_z} \overline{W}_i \tilde{\theta} \tag{23}$$

where $\tilde{\theta}(t) = \begin{bmatrix} \tilde{\theta}_x^T & \tilde{\theta}_z^T \end{bmatrix}^T \in \mathbb{R}^{16}$ and $\overline{W}_i(t) = \begin{bmatrix} W_{xi} & -\hat{P}_i W_{zi} \end{bmatrix} \in \mathbb{R}^{3\times16}$. Generalizing and rewriting (23) for n feature points gives

$$\tilde{P} = L\overline{W}\tilde{\theta}, \tag{24}$$

where $\tilde{P}(t) \in \mathbb{R}^{3n}$, represents the pixel prediction error vector and is given as

$$\tilde{P} = \left[\tilde{P}_1^T,\ \tilde{P}_2^T,\ \cdots,\ \tilde{P}_n^T \right]^T \in \mathbb{R}^{3n}. \tag{25}$$

In (24), the matrix $L(t) \in \mathbb{R}^{3n\times3n}$ is defined as

$$L = diag\left\{ \gamma_1, \gamma_1, \gamma_1, \cdots, \gamma_n, \gamma_n, \gamma_n \right\} \tag{26}$$

where $\gamma_1 = \frac{1}{W_{z1}\theta_z}$ and $\gamma_n = \frac{1}{W_{zn}\theta_z}$. Also, $\overline{W}(t) \in \mathbb{R}^{3n\times16}$ is defined as

$$\overline{W} \triangleq \begin{bmatrix} \overline{W}_1 & \overline{W}_2 & \cdots & \overline{W}_n \end{bmatrix}^T \tag{27}$$

while $\tilde{\theta}(t) \in \mathbb{R}^{16}$ is the parameter estimation error vector.

B. Estimator Design

Based on the stability analysis, the estimation law $\dot{\hat{\theta}}(t)$ is defined as

$$\dot{\hat{\theta}} \triangleq Proj\left\{\alpha\Gamma\overline{W}^T\widetilde{P}\right\} \tag{28}$$

where $Proj\{\cdot\}$ is defined in [22], and $\alpha(t)$ is a positive definite scalar constant defined as

$$\alpha \triangleq 1+\sigma \tag{29}$$

where $\sigma \in \mathbb{R}^+$ is a constant. The projection is employed to avoid singularities that might arise due to the presence of z_i in the denominator of (5). In (28), $\Gamma(t) \in \mathbb{R}^{p\times p}$ is the least squares estimation gain defined as

$$\frac{d}{dt}\left\{\Gamma^{-1}(t)\right\} \triangleq 2\overline{W}^T\overline{W} \tag{30}$$

where $\Gamma(t_0)$ is positive definite and symmetric, ensuring $\Gamma(t)$ is also positive definite and symmetric. Rearranging (10) yields $M \in \mathbb{R}^{3\times 4}$, which is of the form

$$M = A\left[\begin{array}{c} R, T \end{array}\right] \tag{31}$$

and contains all the unknown camera calibration parameters. From (14), it can be seen that the unknown constant vector θ_x contains all the elements of M, thus $\hat{\theta}_x(t)$ will provide an estimate of M. From [23], by redefining M as follows

$$M = \left[\begin{array}{c} B, b \end{array}\right] = \left[\begin{array}{c} AR, AT \end{array}\right] \tag{32}$$

it can be seen that

$$B = AR \quad b = AT \tag{33}$$

where $B \in \mathbb{R}^{3\times 3}$ and $b \in \mathbb{R}^3$. From the definition of $B \in \mathbb{R}^{3\times 3}$ in (33), as seen in [23], the following property can be noted

$$K = BB^T = AR\left(AR\right)^T = AA^T \tag{34}$$

which gives

$$K = AA^T = \left[\begin{array}{ccc} a_{11}^2+a_{12}^2+a_{13}^2 & a_{12}a_{22}+a_{13}a_{23} & a_{13} \\ a_{22}a_{12}+a_{13}a_{23} & a_{22}^2+a_{23}^2 & a_{23} \\ a_{13} & a_{23} & 1 \end{array}\right]. \tag{35}$$

Note that $\hat{\theta}_x(t)$ may be estimated upto a scale factor. In this case, M is normalized such that $K_{33}=1$ (i.e divide M by $\sqrt{K_{33}}$ where K_{ij} represents the element in the i^{th} row and j^{th} column of the K matrix). Solving for all the individual elements in the K matrix, we get

$$\begin{array}{cc} a_{13} = K_{31} & a_{23} = K_{32} \\ a_{22} = \left|\sqrt{K_{22}-a_{23}^2}\right| & a_{12} = \frac{K_{21}-a_{13}a_{23}}{a_{22}} \\ a_{11} = \left|\sqrt{K_{11}-a_{12}^2-a_{13}^2}\right|. & \end{array} \tag{36}$$

The equations in (36) allow for the entire intrinsic camera calibration matrix to be determined. From (33) we can see

$$R = A^{-1}B \quad T = A^{-1}b \tag{37}$$

Thus, substituting R computed in (37) into (13), the extrinsic rotation matrix can be estimated, and subsequently from (11) and the expression for T in (37), the extrinsic translational vector can also be estimated.

C. Stability Analysis

Theorem 1: The update law defined in (28) ensures that $\left\|\tilde{\theta}(t)\right\| \to 0$ as $t \to \infty$ provided the following persistent excitation conditions as seen in [24] hold,

$$\gamma_{i_1}I_{nq} \leq \int_{t_0}^{t_0+T}\overline{W}^T(\tau)\overline{W}(\tau)\,d\tau \leq \gamma_{i_2}I_{nq} \tag{38}$$

where $\gamma_i \in \mathbb{R}\forall i=1,\ldots,n$ are positive constant and $I_{nq} \in \mathbb{R}^{nq\times nq}$ is the identity matrix.

Proof: See [22] which has a similar result. ■

Remark: *By using time-varying trigonometric functions with multiple frequencies to represent the position of the mechanical system, it can be shown from the techniques described in [20] that the persistent excitation condition is satisfied.*

D. Scale Factor Estimation

Since $\hat{\theta}_x(t)$ is estimated upto a scale factor λ, M is also estimated upto a scale factor. Thus we can write (31) as

$$M = \lambda A\left[\begin{array}{c} R, T \end{array}\right] \tag{39}$$

From (32) we can see that,

$$B = \lambda AR. \tag{40}$$

Using the expression in (40) for B, (34) can be rewritten as,

$$K = BB^T = \lambda^2 AR(AR)^T = \lambda^2 AA^T \tag{41}$$

However, we know that K_{33} must be 1, so the scale factor can be determined to be

$$\lambda^2 = K_{33}, \tag{42}$$

which results in

$$\lambda = \sqrt{K_{33}}. \tag{43}$$

Note that K_{33} will always be positive since $K = BB^T$.

IV. Simulation Results

In order to evaluate the effectiveness of the proposed estimation algorithm, a numerical simulation was performed. Twelve static feature points with known Euclidean coordinates with respect to the world frame WF were selected as

$$\begin{array}{ll} X_{f1} = \left[\begin{array}{ccc} 0 & 1 & 1 \end{array}\right]^T & X_{f7} = \left[\begin{array}{ccc} 0.5 & 1 & 1 \end{array}\right]^T \\ X_{f2} = \left[\begin{array}{ccc} 0 & 0.5 & 1 \end{array}\right]^T & X_{f8} = \left[\begin{array}{ccc} 0.5 & 0.5 & 1 \end{array}\right]^T \\ X_{f3} = \left[\begin{array}{ccc} 0 & 0 & 1 \end{array}\right]^T & X_{f9} = \left[\begin{array}{ccc} 0.5 & 0 & 1 \end{array}\right]^T \\ X_{f4} = \left[\begin{array}{ccc} 1 & 1 & 1 \end{array}\right]^T & X_{f10} = \left[\begin{array}{ccc} 0.75 & 1 & 1.5 \end{array}\right]^T \\ X_{f5} = \left[\begin{array}{ccc} 1 & 0.5 & 1 \end{array}\right]^T & X_{f11} = \left[\begin{array}{ccc} 0.75 & 0.5 & 1.5 \end{array}\right]^T \\ X_{f6} = \left[\begin{array}{ccc} 1 & 0 & 1 \end{array}\right]^T & X_{f12} = \left[\begin{array}{ccc} 0.75 & 0 & 1.5 \end{array}\right]^T. \end{array}$$

The equations that described the position of the mechanical system were

$$\begin{array}{l} q_b = \left[\begin{array}{ccc} -0.1\cos(t) & 0.1\sin(t) & 0.2\cos(0.5t) \end{array}\right]^T m \\ \theta_b = \left[\begin{array}{ccc} -0.05\cos(0.2t) & 0.1\sin(0.1t) & 0 \end{array}\right]^T rad \end{array} \tag{44}$$

where $q_b(t) \in \mathbb{R}^3$ and $\theta_b(t) \in \mathbb{R}^3$ represent the robot end-effectors linear and angular positions respectively. These functions governing position were found to satisfy the persistent excitation condition described in (38). Additionally, the camera's target intrinsic calibration matrix and external calibration parameters were taken to be

$$A = \begin{bmatrix} 800 & 1 & 300 \\ 0 & 800 & 200 \\ 0 & 0 & 1 \end{bmatrix} \quad R_c = \begin{bmatrix} 1 & 0 & 0 \\ 0 & 1 & 0 \\ 0 & 0 & 1 \end{bmatrix}$$
$$X_c = \begin{bmatrix} 1 & 0 & 0 \end{bmatrix}^T. \tag{45}$$

Two simulation cases were considered, the first without and the second with additive pixel coordinate noise. In case 2, a Gaussian distributed random number generator was used to simulate the noise signal.

A. Simulation without pixel noise

In this case, the gains which gave the fastest convergence were $\alpha = 50$, while the initial value for Γ was $\Gamma(t_0) = 3I_{16}$, where I_{16} represents a 16×16 identity matrix. The scale factor was determined as $\lambda = 0.0186576$. As seen in Figures 3, 4 and 5, the estimation errors converge close to zero resulting in the following estimates for the intrinsic and extrinsic camera calibration parameters

$$\hat{A} = \begin{bmatrix} 795.2 & 2.386 & 297.9 \\ 0 & 795.2 & 193.9 \\ 0 & 0 & 1 \end{bmatrix}$$
$$\hat{R}_c = \begin{bmatrix} 0.9987 & 0 & 0 \\ 0 & 0.9996 & 0 \\ 0 & 0 & 1 \end{bmatrix}$$
$$\hat{X}_c = \begin{bmatrix} 0.9927 & -0.0184 & -0.0103 \end{bmatrix}^T. \tag{46}$$

It is noted that the estimates are all within a percentage error range of 1% except for A_{23} which falls at 3%.

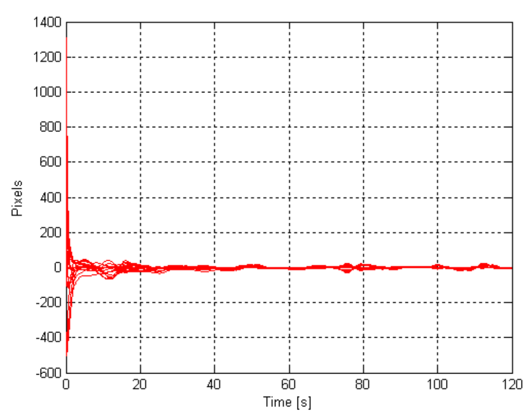

Fig. 3. Pixel coordinate estimation error.

B. Simulation with additive pixel noise

In this case, a variance of 0.2 was used that resulted in a noise signal of upto 2 pixels being added to the actual pixel position estimation.it can be seen from Figures 6, 7 and 8

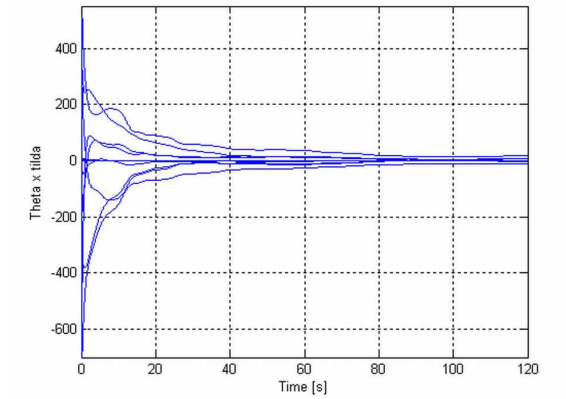

Fig. 4. θ_x parameter estimation error.

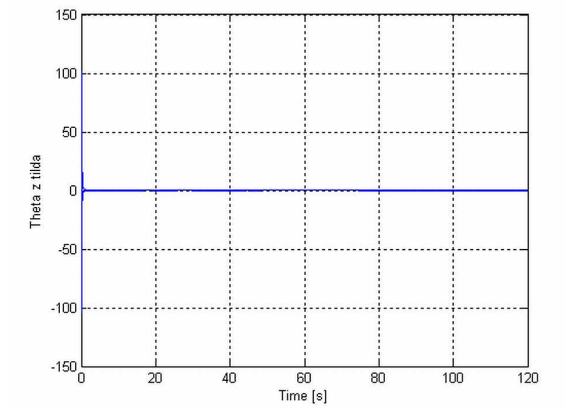

Fig. 5. θ_z parameter estimation error.

that the algorithm takes longer to converge but the noise does not have a significant effect on the estimator which continues to be adequately accurate. The gains which resulted in the fastest convergence times in this case were the same as the case without pixel noise. The scale factor was found to be $\lambda = 0.053239$. Here, the estimated intrinsic and extrinsic camera calibration parameters are

$$\hat{A} = \begin{bmatrix} 812.5 & -4.945 & 305.2 \\ 0 & 812 & 201.2 \\ 0 & 0 & 1 \end{bmatrix}$$
$$\hat{R}_c = \begin{bmatrix} 1 & 0 & 0 \\ 0 & 0.9998 & 0 \\ 0 & 0 & 0.9997 \end{bmatrix}$$
$$\hat{X}_c = \begin{bmatrix} 0.9961 & -0.032 & -0.013 \end{bmatrix}^T. \tag{47}$$

In this case the estimated values fall within 3% of the target values. This demonstrates the robustness of our proposed algorithm.

It should be noted that the final estimated values provided here for both simulations are the average of the last 10 seconds of the simulation to allow for any slight changes that occur as the pixel coordinate estimates vary.

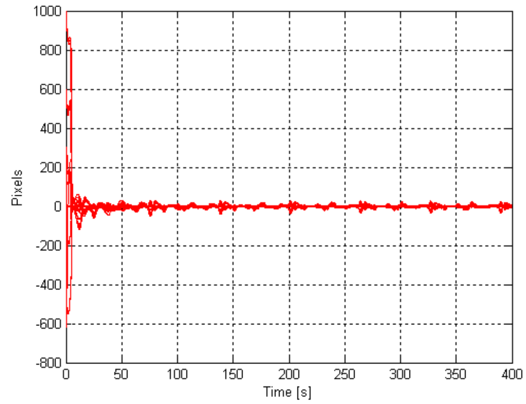

Fig. 6. Pixel coordinate estimation error with additive noise.

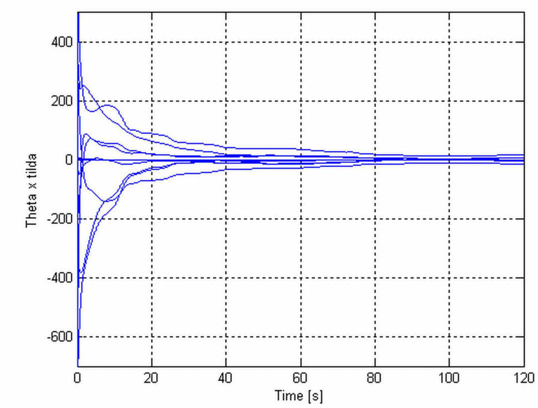

Fig. 7. θ_x parameter estimation error with pixel noise.

V. CONCLUSION

In this paper, a position-based self-calibration technique was developed. To account for the structure of the parameterized pixel coordinate equation, a novel prediction error methodology was outlined along with a least squares-based estimation law. To avoid issues with singularities that could appear due to the depth parameters appearing in the denominator of the pixel equation, a parameter projection formula was employed. A Lyapunov-based stability analysis was utilized to ensure all estimation objectives were achieved.

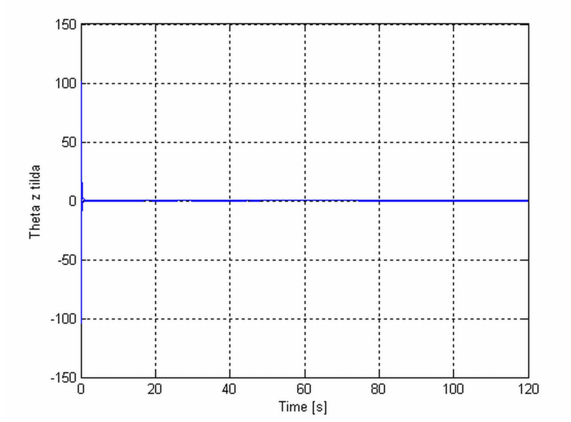

Fig. 8. θ_z parameter estimation error with pixel noise

REFERENCES

[1] O. Faugeras, *Three-Dimensional Computer Vision*. Cambridge, MA: MIT Press, 1993.

[2] Y. C. Shiu and S. Ahmad, "Calibration of wrist mounted sensors by solving the homogenous transform equations of the form ax=xb," *IEEE Trans. Robot. Automat.*, vol. 5, no. 1, pp. 16–29, Feb. 1989.

[3] G. Young, T.-H. Hong, M. Herman, and J. Yang, "Kinematic calibration of an active camera system," in *Proc. IEEE Conf. Comp. Vision and Pattern Recognition*, Champaign, IL, 1992, pp. 748–751.

[4] F. Park and B. Martin, "Robot sensor calibration," *IEEE Trans. Robot. Automat.*, vol. 10, no. 5, pp. 717–721, Oct. 1994.

[5] S. Remy, M. Dhome, J. Lavest, and N. Daucher, "Hand-eye calibration," in *Proc. IEEE/RSJ Int. Conf. Intell. Robots Syst.*, Grenoble, Switzerland, 1997, pp. 1057–1065.

[6] M. Li, "Kinematic calibration of an active head-eye system," *IEEE Trans. Robot. Automat.*, vol. 14, no. 1, pp. 153–158, Feb. 1998.

[7] F. Dornaika and R. Horaud, "Simultaneous robot-world and hand-eye calibration," *IEEE Trans. Robot. Automat.*, vol. 14, no. 4, pp. 617–622, Aug. 1998.

[8] K. Strobl and G. Hirzinger, "Optimal hand-eye calibration," in *Proc. IEEE/RSJ Int. Conf. Intell. Robots Syst.*, Beijing, China, 2006, pp. 4647–4653.

[9] Z. Zhao and Y. Liu, "Hand-eye calibration based on screw motions," in *Proc. IEEE Conf. Pattern Recognition*, Hong Kong, China, 2006, pp. 1022–1026.

[10] D. C. Brown, "Close-range camera calibration," *Photogrammetric Engineering*, vol. 37, pp. 855–866, 1971.

[11] W. Faig, "Calibration of close-range photogrammetry system: Mathematical formulation," vol. 41, no. 12, pp. 1479–1486, December 1975.

[12] Z. Zhang, "A flexible new technique for camera calibration," *IEEE Trans. Pattern Anal. Machine Intell.*, vol. 22, no. 11, pp. 1330–1334, November 2000.

[13] G. Stein, "Accurate internal camera calibration using rotation, with analysis of sources of error," in *Proc. IEEE Conf. Computer Vision*, Cambridge, MA, 1995, pp. 230–236.

[14] Y. Nakazawa, T. Komatsu, and T. Saito, "A simple cue-based method for camera calibration and 3-d shape measurement with a single moving camera," in *Proc. IEEE Conf. Image Processing*, Cambridge, MA, 1996, pp. 293–296.

[15] J. Frahm and R. Koch, "Camera calibration with known rotation," in *Proc. IEEE Conf. Computer Vision*, Nice, France, 2003, pp. 1418–1425.

[16] S. Maybank and O. Faugeras, "A theory of self-calibration of a moving camera," *International Journal of Computer Vision*, vol. 8, no. 2, pp. 123–151, Aug. 1992.

[17] R. Tsai, "A versatile camera calibration technique for high-accuracy 3d machine vision metrology using off-the-shelf tv cameras and lenses," *IEEE Journal of Robotics and Automation*, vol. 3, no. 4, pp. 323–344, Aug. 1987.

[18] J. Heikkila and O. Silven, "Accurate camera calibration with new minimizing function," in *Proc. IEEE Conf. Computer Vision Pattern Recognition*, San Juan, Mexico, 1997, pp. 1106–1112.

[19] J. Batista, H. Araujo, and A. D. Almeida, "Iterative multi-step explicit camera calibration," in *Proc. IEEE Conf. Computer Vision*, Bombay, India, 1998, pp. 709–714.

[20] S. Sastry and M. Bodson, *Adaptive Control: Stability, Convergence and Robustness*. Englewood Cliffs, NJ: Prentice Hall, 1989.

[21] M. W. Spong and M. Vidyasagar, *Robot Dynamics and Control*. New York, NY: John Wiley and Sons, 1989.

[22] E. Tatlicioglu, D. M. Dawson, and B. Xian, "Adaptive visual servo regulation control for camera-in-hand configuration with a fixed-camera extension," in *Proc. IEEE Int. Conf. Decision and Control*, New Orleans, LA, 2007, pp. 2339–2344.

[23] G. Medioni and S. B. Kang, *Emerging Topics in Computer Vision*. Upper Saddle River, NJ: Prentice Hall, 2005.

[24] J. J. E. Slotine and W. Li, *Applied Nonlinear Control*. Englewood Cliffs, NJ: Prentice Hall, 1991.